Aerospace Science and Technology 42 (2015) 31–38

Contents lists available at ScienceDirect

Aerospace Science and Technology

www.elsevier.com/locate/aescte

Hierarchical modeling and optimization of camber morphing airfoil

Senthil Murugan *, B.K.S. Woods, M.I. Friswell *

College of Engineering, Swansea University, Singleton Park, Swansea SA2 8PP, UK

ARTICLE INFO

Article history:
Received 9 May 2013
Received in revised form 1 August 2014
Accepted 25 October 2014
Available online 14 January 2015

Keywords:
Hierarchical models
Camber morphing airfoil
Compliant structure
Curvilinear fiber composite
Multi-objective optimization

ABSTRACT

A variable camber morphing airfoil with compliant ribs and flexible composite skins is studied in a hierarchical modeling framework. The key requirements of a variable camber morphing airfoil are the flexible skin, compliant internal structure and a lightweight actuation system. A biologically inspired, internal structure is adapted to produce continuous camber morphing. The conflicting requirements of the morphing skin, namely low in-plane stiffness and high out-of-plane bending stiffness, are met by designing the composite with curvilinear fiber paths. A coupled aeroelastic simulation and optimization of the proposed 2-D morphing airfoil is computationally complex. Hierarchical computational models of the morphing airfoil are used to decouple the complaint ribs and airfoil skin. In the first level of hierarchy, a fluid-structure interaction is performed with the homogenized beam model of the compliant rib structure and 2-D panel method. In the second level, a finite element model of the camber morphing skin is developed with representative boundary conditions. A multi-objective optimization framework is developed to find the optimal curvilinear fiber paths of the morphing skin to meet the airfoil geometric shape and actuation requirements of the first level. The optimal results show that a significant camber variation and significant changes in aerodynamic properties can be achieved with the compliant skin and airfoil structure considered in this study. The hierarchical modeling framework of the camber morphing airfoil discussed in this paper enhances theoretical understanding of each sub-system and reduces the computational costs.

1. Introduction

Morphing wing concepts aim to enhance the aircraft performance by designing wings that can be morphed to optimal shape of each flight condition [4,30]. Morphing wings, in general, can be categorized based on the scale of morphing as large, medium and small scale morphing concepts [30]. The variable camber airfoil is a small-to-medium scale morphing concept that requires the wing skins and rib or internal structures to undergo a strain of around 2–3% [11].

The camber of an airfoil has a significant impact on the aerodynamic forces it will generate under fluid flow [1,2,27,29]. Generally, the variable camber of an airfoil is realized through the use of discrete trailing edge flaps [6]. However, the presence of a sharp and discrete change in camber leads to a significant increase in drag over the baseline airfoil, particularly at high lift coefficients. Considerable research has focused on developing an airfoil with smooth and continuous camber change, defined as a camber morphing airfoil, as an alternative to discrete flaps that can lead to significant reduction in the drag [4]. The main challenges of a successful camber morphing airfoil are: 1) flexible airfoil skins, 2) adaptive internal structures, and 3) lightweight actuation systems. From a theoretical perspective, the computational modeling and simulation of these novel reconfigurable aero-servo-elastic systems is a major challenge [9]. A brief review of studies focused on novel structural concepts and modeling issues of camber morphing airfoils are discussed in the following paragraphs.

The multi-functional aspects of morphing airfoil skins result in conflicting structural requirements of low in-plane stiffness and high out-of-plane bending stiffness, a highly anisotropic nature [24,31]. Most studies on camber morphing airfoils, primarily focused on UAVs, consider the skin to be made of silicone rubber, elastomeric and flexible isotropic materials [4,5]. A detailed review on novel morphing skins with highly anisotropic characteristics are given in Ref. [31]. Coutu et al. [7] studied the design of an active extrados structure for an experimental Morphing Laminar Wing (MLW). The upper skin of the MLW, made of composite laminate, is morphed to match the optimal target profiles. The number of plies of the flexible extrados and the number of actuators are optimized to maximize the aerodynamic and mechanical performance of the airfoil. However, the composite laminate is considered to be

* Corresponding authors. Tel.: +44 (0)1792 602969; fax: + 44 (0)1792 295676.
E-mail addresses: s.m.masanam@swansea.ac.uk (S. Murugan), m.i.friswell@swansea.ac.uk (M.I. Friswell).

http://dx.doi.org/10.1016/j.ast.2014.10.019
1270-9638/

made of uni-directional plies. Murugan et al. [24] proposed a flexible fiber reinforced composite skin with a optimal distribution of volume fraction of fibers. The numerical results showed that the ratio of in-plane flexibility to bending stiffness can be improved by 30–40% compared to composites with a uniform fiber distribution. The main limitation of these composites is that the fibers have to be uni-directional and orthogonal to the morphing direction to retain the low in-plane stiffness. Thuwis et al. [32] studied the application of variable stiffness composite skins for the leading edge of a camber morphing wing. However, a scaled parameter accounting for the variation of stiffness in space is used instead of the direct variation of the fiber angles or thickness along the space. In a recent study, Murugan and Friswell [20] proposed a flexible composite skin with curvilinear fibers, in contrast to straight fiber composites, for the variable chord airfoil. However, to the authors' knowledge, no study has focused on the use of composite with curvilinear fibers for a variable camber airfoil [25]. The Fish Bone Active Camber (FishBAC) concept introduced by Woods and Friswell [34] is coupled with the curvilinear fiber composite skin to realize the 2-D camber morphing airfoil proposed in this study.

In this paragraph, the previous studies on modeling issues of camber morphing wings are discussed. In general, a commercial finite element program is used to model the 2-D airfoil structural model and aerodynamic loads are evaluated with linear potential flow theory at multiple morphed states [8,19,28,37]. Aeroelastic simulation is performed based on weak coupling. Actuation is considered via external forces acting on the structural model. A direct coupling of the 3-D or 2-D structural finite element models of the wings with aerodynamic codes can result in a high computational cost, lacks the understanding of each sub-system and, any optimization of each sub-system can be expensive [32]. A few studies have focused on analytical or numerical modeling of camber morphing airfoils. Gandhi and Inthra [11] studied the desirable attributes of the flexible skin of a variable camber morphing wing with a numerical model of the 2-D airfoil. De Gaspari and Ricci [9] proposed a two-level approach for the optimal design of camber morphing wings. In the first level, an optimization is performed to identify the optimal aerodynamic shapes of the morphing airfoil. In the second optimization level, an ad hoc topology optimization tool is used to synthesize an optimal compliant structure that adapts to the optimal shapes of the first level. However, the design or feasibility of anisotropic airfoil skins and actuation systems are not defined in both of the studies [9,11].

The aim of this work is to develop a variable camber trailing edge airfoil with compliant structures and study these concepts in a hierarchical modeling framework. The FishBAC morphing structure and a variable stiffness skin based on curvilinear fiber composites is proposed. A two-level hierarchical framework of the camber morphing 2-D airfoil is developed. In the first level, a homogenized beam model of the compliant rib structure is developed and 2-D panel method code is used to evaluate the aerodynamic loads for a given actuation. In the second level, the structural model of the skin is developed with representative boundary conditions of the morphing wing. The aerodynamic loads and deformation requirements from the first level are used to optimize the skin. A multi-objective optimization framework, at the second level, is used to find optimal curvilinear fiber paths of the composite skin.

2. Hierarchical modeling of the airfoil

A variable camber 2-D airfoil employing the FishBAC morphing concept that is representative of a typical rotor blade or a UAV wing is considered in this study and shown in Fig. 1. The airfoil has a stiff D-spar at the leading edge and an active morphing structure at the trailing edge. In the early stages of conventional wing

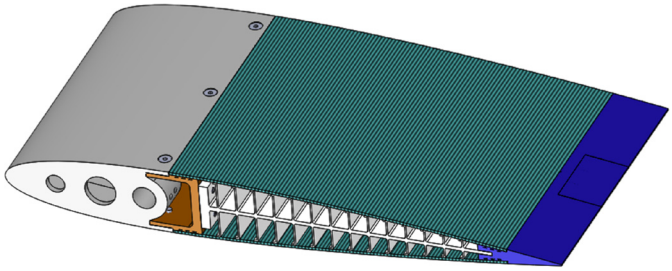

Fig. 1. Morphing airfoil with a compliant internal structure and flexible skin.

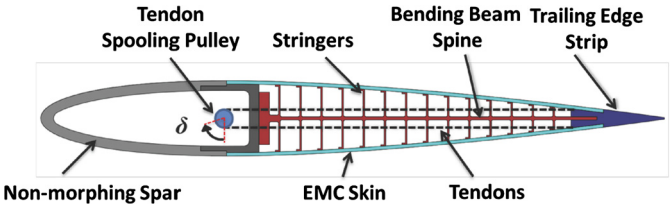

Fig. 2. FishBAC compliant structure.

design process, hierarchical structural and aerodynamic models of the wing are developed to study each sub-system and to reduce the computational effort [16,27]. From the structural perspective, a high-aspect ratio 3-D wing (non-morphing) is modeled and analyzed with a minimum of two levels of hierarchy [33]. At a lower level in the hierarchy, a structural analysis is performed with the 2-D cross-sectional model of the wing. At a higher level in the hierarchy, an aeroelastic analysis is performed based on the 1-D beam model constructed with cross-sectional properties from the lower level [21–23]. This process is generally applicable for a wing with fixed cross-sectional geometry. However, in the case of camber morphing airfoils, the geometry of the cross-section changes by an externally applied actuation force. This introduces additional degrees of freedom along the chordwise direction of the airfoil. Therefore, additional hierarchical models are needed to capture the morphing behavior of airfoil cross-section which are discussed in the following sections. The 2-D variable camber airfoil discussed in this paper is split into the variable camber internal structure and flexible skins. The modeling of the variable camber internal structure is discussed in Section 3. The modeling and optimization of the morphing skin with curvilinear fiber composites is discussed in Section 4.

3. Variable camber structure

An adaptive internal structure for the variable camber airfoil, homogenized model and fluid–structure interaction (FSI) simulation is discussed in this section.

3.1. FishBAC concept

Woods and Friswell proposed a bio-inspired compliant internal structure known as the FishBone Active Camber (FishBAC) structure [34]. This design employs a highly anisotropic structure to create large changes in aerodynamic properties with continuous changes in airfoil camber. A schematic overview of the FishBAC concept is shown in Fig. 2.

The FishBAC structure consists of a thin chordwise bending beam spine with stringers branching off to connect it to a pre-tensioned Elastomeric Matrix Composite (EMC) skin surface. Smooth, continuous bending deflections are driven by a high stiffness, antagonistic tendon system. Actuators mounted in the D-spar drive a tendon spooling pulley through a non-back drivable mechanism (such as a low lead angle worm and worm gear). Rotation

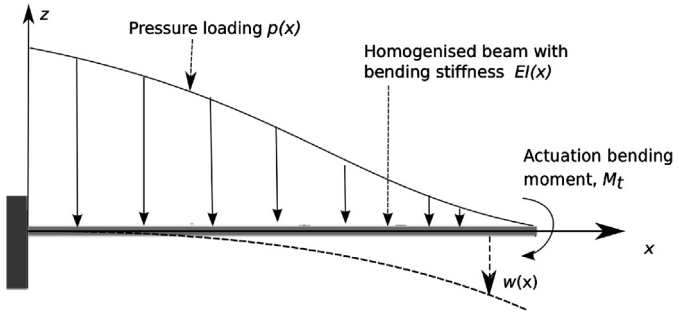

Fig. 3. Homogenized beam representation of the trailing edge aft of the D-spar.

of the pulley creates equal but opposite deflections of the tendons. These differential displacements generate a bending moment on the rigid trailing edge strip, which then induces bending of the trailing edge morphing structure to create large changes in airfoil camber. Since the tendon system is non-back drivable, no actuation energy is required to hold the deflected position of the structure, leading to increased operational efficiency. The FishBAC concept creates large camber deflections with minimal actuation energy requirements through the use of structural and material anisotropy. The spine and stringer core is highly anisotropic, with very low bending stiffness along the chord direction, but high span wise and through-thickness bending stiffness. That is, the bending stiffness corresponding to the camber variation is less while the blade bending stiffness along the span wise direction is high.

3.2. Fluid–structure interaction analysis

This section will provide an overview of the low-fidelity fluid–structure interaction (FSI) analysis developed in the previous work [35]. The FSI is performed with the homogenized model of FishBAC internal structure and an elastomeric skin. The results of FSI analysis, the morphed geometry and aerodynamic pressure loading, are used in this study to design and optimize the flexible airfoil skin with curvilinear fiber composites. The design and optimization of flexible composite skin, presented in the later sections of this study, is not coupled into FSI analysis. However, the results of FSI are used to provide a reasonable, representative geometry of the camber morphed airfoil and the corresponding aerodynamic pressure distribution.

The idealized beam model of the FishBAC internal structure is described in the following paragraph. The trailing edge portion of the FishBAC internal structure, aft of the D-spar, is homogenized as a cantilever beam as shown in Fig. 3. A fully coupled partitioned fluid–structure interaction (FSI) analysis is used to evaluate the aerodynamic loads which then later used in the flexible skin designs [35]. The FSI is performed with parameters of 0.3 m chord and 10 degrees angle of attack. Full details of the operating point, aerodynamic coefficients of the baseline and morphed airfoil are given in Table 1. The FSI code finds the converged static equilibrium deflections of the structure under internal actuation and external aerodynamic loading using a fixed point iteration scheme [35]. The algorithm of the FSI code will be briefly overviewed here to provide sufficient understanding of the aerodynamic results used in the optimal design of skins.

3.2.1. Hierarchical level II: structural model of compliant mechanism

The compliant internal structure of the FishBAC airfoil is modeled using a simple Euler–Bernoulli beam formulation. The bending beam spine is modeled as a single element beam with the distributed bending stiffness (EI_b) in the chord direction x:

$$EI_b = \frac{E_b}{12} b h(x)^3 \tag{1}$$

Table 1
FishBAC FSI solution parameters.

Parameter	Value
Baseline airfoil	NACA 0012
Chord	0.3 m
Reynolds no.	400,000
P_{atm}	101,325 Pa
Angle of attack	10 deg
Drive pulley rotation	30 deg
Lift coefficient, c_l (baseline)	0.991
Drag coefficient, c_d (baseline)	0.0284
Lift coefficient, c_l (morphed)	1.70
Drag coefficient, c_d (morphed)	0.061

where E_b is the elastic modulus, b the width, and h the thickness of the spine. The effective bending stiffness of the skin (EI_s) about the neutral axis of the structure is then found using the parallel axis theorem

$$EI_s = E_s\left[\frac{1}{12} b t_s^3 + b t_s y_s(x)^2\right] \tag{2}$$

where E_s is the elastic modulus, t_s the thickness, and y_s the distance from the neutral axis of the skin. The total bending stiffness of the structure is then found as the linear superposition of the skin and spine stiffness:

$$EI_{tot} = EI_b + EI_s \tag{3}$$

The relationship between applied loading $p(x)$ and vertical spine displacement $w(x)$ is then found by integrating the Euler–Bernoulli equation

$$EI\frac{d^4 w(x)}{dx^4} = p(x) \tag{4}$$

For boundary conditions, the inboard end of the spine is assumed clamped with the trailing edge free. Each step in the fixed point iteration produces a chordwise distribution of spine bending deflection. The outer profile of the deformed FishBAC structure is then found by superimposing the thickness distribution of a NACA 0012 airfoil onto the spine deflection.

3.3. Aerodynamic model

The effects of aerodynamic loading on the structure are included through the use of the viscous panel method code, XFOIL [36]. At each iteration step, the aerodynamic pressure acting on the FishBAC airfoil is calculated using the aerodynamic operating point and the current estimate of the deformed outer profile. Local out-of-plane deformations of the skin between stringers are not included in this level of the analysis. The resulting pressure distributions are therefore only valid for small deformations of the skin.

3.4. Actuation model

The tendon driven actuation is included in the FSI analysis as a discrete moment generator on the trailing edge that depends on prescribed initial actuation displacements and deformation derived strains. The tendons are modeled as linear elastic axial members with an initial prescribed displacement and no bending stiffness. The initial displacement is due to spooling pulley rotation through a prescribed angle according

$$\Delta l_{t,0} = \delta r_p \tag{5}$$

where the spooling pulley rotation angle is the prescribed actuation variable, and r_p is the radius of the spooling pulley. While the tendons do not have any bending stiffness of their own, they

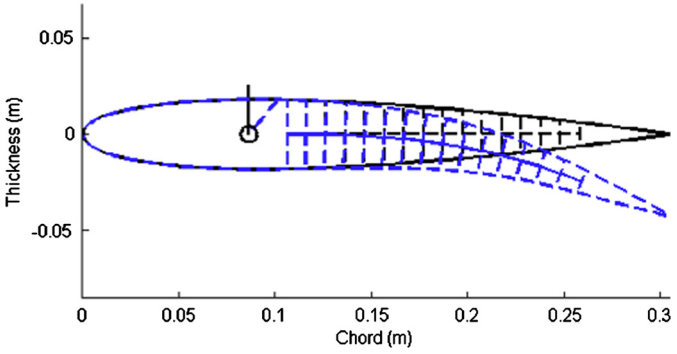

Fig. 4. Undeformed and morphed configuration of the airfoil.

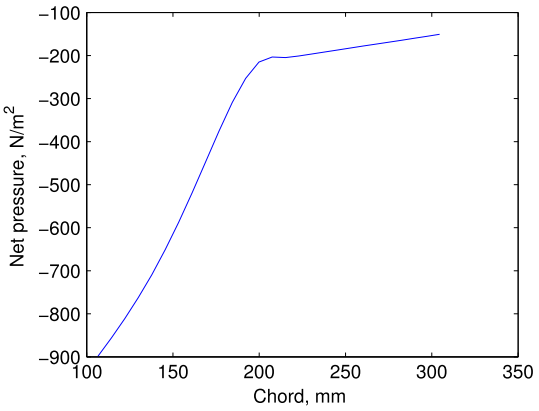

Fig. 5. Aerodynamic pressure loads on the upper skin.

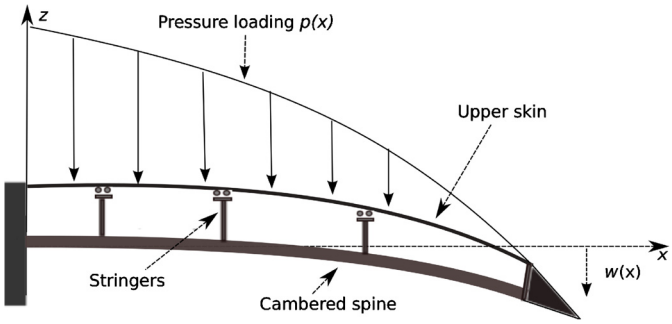

Fig. 6. Boundary conditions of the morphing skin and stringers.

are held at a constant distance from the bending spine as the trailing edge morphs by traveling through small orifices in the stringers. Due to their constant distance from the neutral axis, tendon strains induced by structural bending are also derived from Euler–Bernoulli theory as

$$\Delta l_{t,e} = \int \frac{M_{aero}(x)}{EI_{tot}(x)} y_t dx \tag{6}$$

with M_{aero} being the applied aerodynamic moment and y_t the vertical mounting offset of the tendons at their trailing edge anchor point. The axial stiffness and initial displacement of the tendons will therefore drive the trailing edge deflections by creating a discrete bending moment M_t on the trailing edge strip (where they are anchored) according to

$$M_t = 2y_t \frac{E_t A_t}{L_t}(\Delta l_{t,0} + \Delta l_{t,e}) \tag{7}$$

where E_t is the elastic modulus, A_t the cross-sectional area, and L_t the length of the tendons. The effect of this induced bending moment is included in the integration of the Euler–Bernoulli equation as a discrete moment.

3.5. FSI convergence

The actuation moment, aerodynamic pressure distributions and spine deflections are all highly coupled. Therefore, the FSI code is iterated several times at each design point to achieve convergence. Additionally, since there is a large difference in the magnitude of the aerodynamic and structural stiffnesses, a relaxation parameter is needed to ensure convergence [35]. Convergence is monitored through the magnitude of the spine displacement and the aerodynamic coefficients, with the convergence criteria being met only when the tip deflection, lift coefficient, drag coefficient, and moment coefficient of the FishBAC are found to change less than 2% between iterations. The deformed configuration and net pressure acting on the upper skin are shown in Figs. 4 and 5.

4. Flexible composite skins

The flexible skin for the variable camber airfoil section with a FishBAC internal structure is studied in this section. The out-of-plane deflections (local) of the skin induced by the aerodynamic pressure can play a significant role in altering the flow over the airfoil. Similarly, the increase in actuation power requirements to morph the skin can result in an increase in the weight of the actuation system. Minimizing the power or actuation requirements of morphing systems can result in significant weight savings. Therefore, the objective in this section is to design the skin to minimize the actuation energy while simultaneously minimizing the out-of-plane deflections caused by the aerodynamic pressure.

4.1. Hierarchical level I: morphing skin model

The dimensions of a previously developed FishBAC prototype are used to develop the structural skin model. This structural modeling and analysis of the morphing skin can be considered as level I in the hierarchical modeling of the camber morphing airfoil. The embodiment of the FishBAC internal structure studied, shown in Fig. 2, has 14 stringers along the chordwise direction. The skin between the aft of the D-spar and the trailing edge is modeled as a shell structure that is simply supported over the stringers. The trailing edge and leading edge ends of the skin are modeled as clamped supports. This allows the skin to deform to a new camber shape while retaining a smooth outer aerodynamic profile as shown in Fig. 6.

As shown in Fig. 5, the aerodynamic pressure varies along the chordwise direction. The bending stiffness of the skin along the chordwise direction, between each of the stringers, can also be varied in proportion to the aerodynamic pressure. By varying the fiber angles along the chord, the maximum out-of-plane deflections between the stringers and the actuation energy required to morph the skin can be minimized. In this study, the design of the upper skin is addressed and a similar method can be used to design the lower skin of the airfoil. The theory of curvilinear fiber composites and the multi-objective optimization framework to design the morphing skins are discussed in the following subsections.

4.2. Curvilinear fiber composite model

The fiber paths of curvilinear fiber composites can be defined with various mathematical functions [14,17,20,26]. However, the

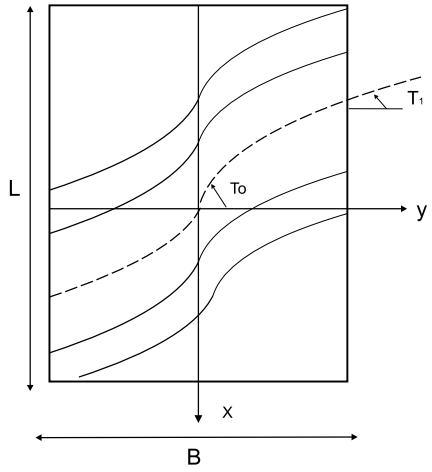

Fig. 7. Curved fiber paths in a composite plate.

selection of fiber paths are limited by manufacturing constraints. Most studies on curved fiber composite define a linear, 1-D variation of a reference fiber path [14,15,20]. This linear variation along the panel direction y, as shown in Fig. 7, can be given as

$$\theta(y) = 2(T_1 - T_o)\left|\frac{y}{B}\right| + T_o \tag{8}$$

where $\theta(y)$ represents the fibre orientation, B denotes the width of the plate, and T_1 and T_0 represent the fiber angles at the edge ($y = B/2$) and middle of the plate ($y = 0$), respectively. This reference fiber path can be repeated along the x direction to manufacture the curvilinear fiber (CVF) composite plate [14]. This fiber path definition of the single ply layer is generally represented as $\langle T_0|T_1\rangle$. The stacking sequence of a balanced symmetric CVF laminate with $2n$ plies can be given as $[\pm\langle T_o^k|T_1^k\rangle_n]_s$. The values of T_0 and T_1 are given in degrees in this study. The constitutive equations of a variable stiffness composite in terms of force resultants (N_x, N_y, and N_{xy}) and moment resultants (M_x, M_y, and M_{xy}), for balanced symmetric laminates are

$$\begin{Bmatrix} N_x \\ N_y \\ N_{xy} \end{Bmatrix} = \begin{bmatrix} A_{11}(x,y) & A_{12}(x,y) & 0 \\ A_{11}(x,y) & A_{22}(x,y) & 0 \\ 0 & 0 & A_{66}(x,y) \end{bmatrix} \begin{Bmatrix} u_{o,x} \\ v_{o,y} \\ u_{o,y} + v_{o,x} \end{Bmatrix} \tag{9}$$

$$\begin{Bmatrix} M_x \\ M_y \\ M_{xy} \end{Bmatrix} = \begin{bmatrix} D_{11}(x,y) & D_{12}(x,y) & D_{16}(x,y) \\ D_{12}(x,y) & D_{22}(x,y) & D_{26}(x,y) \\ D_{16}(x,y) & D_{26}(x,y) & D_{66}(x,y) \end{bmatrix} \begin{Bmatrix} w_{o,xx} \\ w_{o,yy} \\ 2w_{o,xy} \end{Bmatrix} \tag{10}$$

where A_{ij} and D_{ij} are the elements of the in-plane and bending stiffness matrix of the composite plate, respectively [18]. The mid out-of-plane displacement is represented by w and in-plane displacements in the x and y directions are represented by u and v, respectively. The above equations show that the in-plane and out-of-plane displacements depend on A_{ij} and D_{ij}, respectively. The stiffness parameters are given by

$$A_{ij} = \sum_{k=1}^{n} Q_{ij}(z_k - z_{k-1}), \qquad D_{ij} = \sum_{k=1}^{n} \frac{Q_{ij}}{3}\left(z_k^3 - z_{k-1}^3\right) \tag{11}$$

where the Q_{ij}s are the transformed reduced stiffness terms. The terms z_k and z_{k-1} are the upper and lower coordinates of the kth ply, respectively. The above relations show the in-plane stiffness of a CVF laminate is a function of the thickness of the plies ($z_k - z_{k-1}$) and spatial variation of the $Q_{ij}(x, y)$ which in turn is a function of the fiber angle, θ. Similarly, the bending stiffness of the CVF laminate is a function of the spatial variation of fiber angle and the stacking sequence of plies, in addition to the thickness term $(z_k^3 - z_{k-1}^3)$.

4.3. Multi-objective optimization framework

The morphing skin is modeled as a CVF composite plate with the boundary conditions shown in Fig. 6. The skin deformations due to aerodynamic and actuation loads can be solved using numerical methods such as finite element analysis. In this study, the structural analysis is performed with a commercial finite-element analysis tool and the skin is modeled using shell finite elements [3,20]. The skin is considered to be made of a graphite/epoxy balanced symmetric laminate with 16 plies. Each ply has a thickness of 0.01 mm. The structural properties of baseline skin is chosen such that the local deformations of skin will not affect the global aerodynamic performance [11]. The optimization is carried out as a three step process. In the first step, the strain energy required to morph the skin is evaluated. In the second step, the out-of-plane deflections of the skin between the stringers due to the aerodynamic pressure is evaluated. In an outer loop, the strain energy and out-of-plane deflections are minimized in a multi-objective framework.

Initially, the upper skin of airfoil is modeled with zero camber. The change in camber, induced by the actuation, is applied to the initial configuration as specified in Fig. 4. The elastic strain energy stored in the skin due to this deformation is calculated. This strain energy can be considered as an equivalent of actuation energy needed to deflect the skin. Therefore, the first objective function can be given as

$$\text{Minimize,} \quad J_1 = U_{skin} \tag{12}$$

where U_{skin} is the elastic strain energy.

In the second step, the net aerodynamic pressure is applied to the morphed skin configuration of the first step. The global deflection of the morphed airfoil is maintained by the skin, stringer supports and spine as shown in Fig. 4. However, the local deformations of the skin between the stringers can perturb the aerodynamic performance of the morphed airfoil [11]. Therefore, the out-of-plane deflections of skin between the stringers is included in the optimization process. The objective function to minimize the out-of-plane deformation of the skin between the stringers is given as

$$\text{Minimize,} \quad J_2 = \text{Max}\{wl_i\} \quad i = 1, n \tag{13}$$

where wl_i is maximum out-of-plane deflection of ith panel of the skin and n is the number of panels between the stringers of compliant rib.

Now, the objective functions given in Eqs. (12) and (13) are combined to form a multi-objective optimization problem that is defined as

$$\text{Minimize,} \quad J = \left[J_1(X), J_2(X)\right] \qquad X = \left[\langle T_p^0|T_p^1\rangle\right]_s \tag{14}$$

where X is the vector of design variables and p represents the pth ply of the curvilinear fiber composite. The objective functions are non-dimensionalized with the numerical values of a baseline skin made of $\pm 45°$ straight fiber laminates. In the optimization process, the fiber paths are considered to vary along the chordwise direction of the airfoil. The fiber paths of the 14 skin panels are given by Eq. (8) and are represented with two design variables T_0 and T_1. Therefore, the curvilinear fiber composite made of a balanced

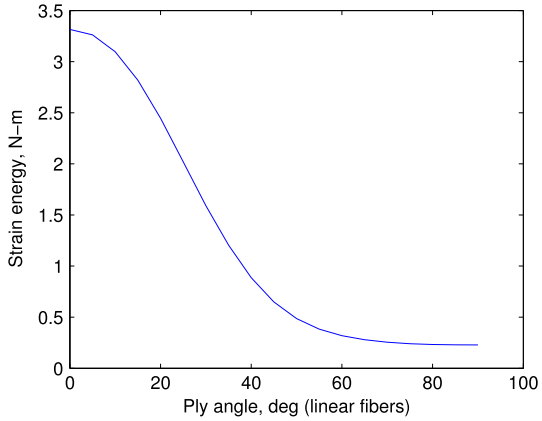

Fig. 8. Strain energy variation with respect to fiber angle (straight fibers).

symmetric laminate with 16 plies results in 8 design variables that are given below.

$$X = \left[\pm\langle T_1^0|T_1^1\rangle, \pm\langle T_2^0|T_2^1\rangle, \pm\langle T_3^0|T_3^1\rangle, \pm\langle T_4^0|T_4^1\rangle\right] \tag{15}$$

Before the optimization process, the elastic strain energy of the skin, for a span of 10 mm, due to camber morphing is calculated for a laminate with straight fibers for a span of 10 mm. The ply angles (straight fibers) of the skin are varied from 0 to 90° and shown in Fig. 8. The strain energy (SE) varies from 3.25 to 0.25 J (for a span of 10 mm) as the angle varies from 0 to 90°. The SE shows a much smaller value (0.25 J) for ply angles greater than 45° compared to 0°. This is because of the fiber directions in relation to the boundary conditions of the skin. A servo actuator capable of providing 2.5 J with dimensions to fit inside the D-spar of the FishBAC is used as an actuator in the prototype.

4.4. Optimal curvilinear fiber results

Genetic algorithms (GA) are commonly used in the optimal design of constant stiffness and variable stiffness composite laminates [12,13,17]. The multi-objective genetic algorithm based on the non-dominated sorting genetic algorithm (NSGA-II) is used in this study to obtain the Pareto-optimal solutions [10]. A detailed explanation of the optimization of curved fiber composites with NSGA-II is given in Refs. [17,20]. A multi-objective optimization is performed with the objective functions and design variables given in Eqs. (14) and (15). The Pareto-optimal results are shown in Fig. 9. The Pareto front shows five optimal solutions for which the objective functions J_1 and J_2 are simultaneously reduced from their baseline values. Further, the Pareto front shows an almost linear increase in the out-of-plane deformation while the elastic strain energy is minimized. In Table 2, the five Pareto-optimal solutions for which the strain energy and out-of-plane deformation are minimized simultaneously are given. These optimal solutions, as shown in Fig. 9, show a reduction of 6 to 32% in the strain energy while the out-of-plane deformations are reduced by 1 to 38%. These results show that curvilinear fiber composites can be used to minimize the actuation energy required to morph the skin while simultaneously minimizing the skin deformation due to aerodynamic loads. As an illustration, the curved fibers corresponding to optimal point 2 in Table 2 are shown in Fig. 10.

Table 2
Pareto-optimal solutions.

No.	Strain energy (% reduction)	Out-of-plane deformation (% reduction)	Curved fiber angles $[\pm\langle T_o^k|T_1^k\rangle_4]$
1	6	38	$[\pm\langle 43\|22\rangle, \pm\langle 72\|66\rangle, \pm\langle 70\|70\rangle, \pm\langle 76\|73\rangle]$
2	10	34	$[\pm\langle 44\|24\rangle, \pm\langle 74\|60\rangle, \pm\langle 69\|73\rangle, \pm\langle 71\|72\rangle]$
3	17	25	$[\pm\langle 44\|30\rangle, \pm\langle 72\|60\rangle, \pm\langle 71\|72\rangle, \pm\langle 73\|72\rangle]$
4	23	19	$[\pm\langle 48\|30\rangle, \pm\langle 78\|61\rangle, \pm\langle 70\|73\rangle, \pm\langle 72\|72\rangle]$
5	32	1.0	$[\pm\langle 51\|37\rangle, \pm\langle 70\|58\rangle, \pm\langle 63\|60\rangle, \pm\langle 72\|73\rangle]$

In Eq. (8), the numerical values of T_n^0 and T_n^1 define the fiber paths to be curved along the direction of chord or span. In general, if the numerical values of T_n^0 and T_n^1 are less than 45°, the fiber paths are almost curved along the chord direction. Similarly, if the values of T_n^0 and T_n^1 are greater than 45°, the fiber paths are curved along the span direction. From the optimal values of T_0 and T_1 given in Table 2, it can be realized that the ply which is away from the neutral axis of the laminate (ply 1) tends to be curved along the chord direction of airfoil while the plies closer to the neutral axis (plies 2, 3 and 4) tend to be curved along the span of the wing. The results of this optimization study show the use of curvilinear fiber composites for camber morphing wing skins can be highly beneficial compared to straight fiber composites. Further, the hierarchical modeling framework of the camber morphing air-

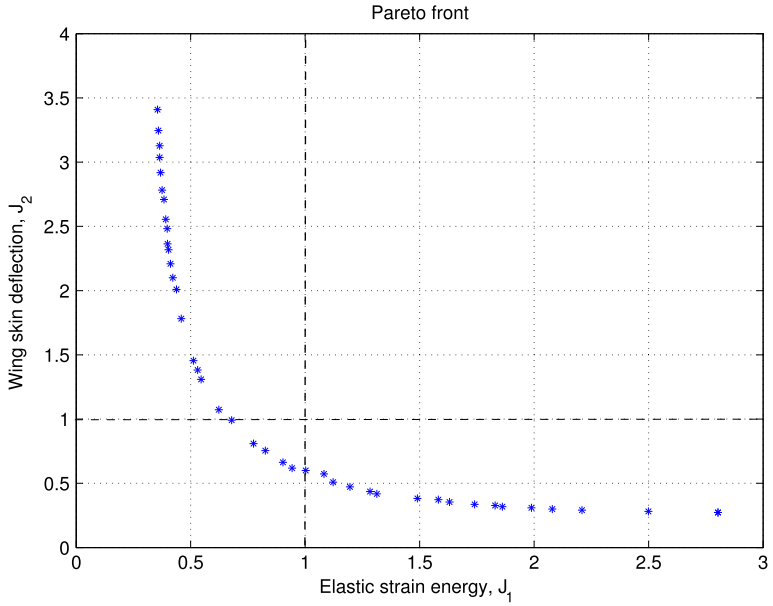

Fig. 9. Pareto-optimal solutions.

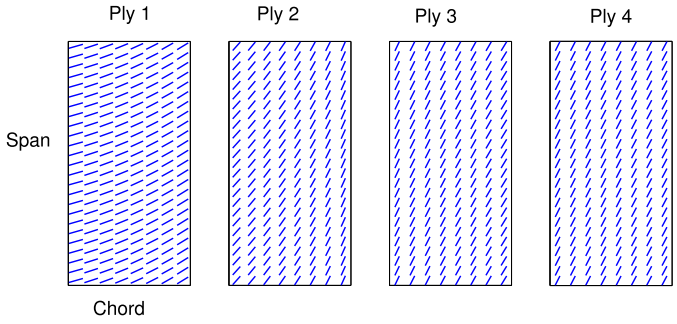

Fig. 10. Optimal curved fiber paths.

foil discussed in this paper enhances theoretical understanding of each sub-system and reduces the computational cost. The optimal designs obtained from the hierarchical modeling framework can also be verified with the high fidelity simulations or wind tunnel tests.

5. Conclusion

A bio-inspired camber morphing airfoil is studied in a hierarchical modeling framework in this paper. A flexible skin based on a curvilinear fiber composite and a compliant internal structure based on FishBone Active Camber is proposed for camber morphing airfoil. A two-level hierarchical modeling of the 2-D morphing airfoil is used to decouple the aeroelastic simulation of the compliant 2-D structure and the skin design optimization. A homogenized beam model of the active compliant structure is presented. An aeroelastic simulation of the 2-D airfoil cross-section is performed with the homogenized beam model. The aerodynamic loads on the morphing skin are obtained for the given actuation force. The aerodynamic loads and camber deformation are used to find the optimal fiber paths for the composite skin. A multi-objective optimization problem is formulated to minimize the actuation energy and out-of-plane deformation of the skin. The Pareto-optimal solutions show considerable reduction in the elastic strain energy and out-of-plane deformations of skin, simultaneously. The plies which are away from the neutral axis of the laminate tend to be curved while the plies near the neutral axis tend to be straight fibers. The optimal results show the curvilinear fibers can be beneficial to meet the conflicting design requirements of camber morphing wing skins. A significant camber variation and hence change in aerodynamic properties can be achieved with the compliant structure considered in this study. The hierarchical modeling proposed in this study successfully decouples the aeroelastic simulation and the skin design optimization. As an alternative to the fully coupled aeroelastic simulation of a morphing structure, this hierarchical modeling allows the designer to establish the mathematical models of the subsystem components, optimize the system with affordable computational cost and enhances the theoretical understanding of each subsystem.

Conflict of interest statement

We wish to confirm that there are no known conflicts of interest associated with this publication and there has been no significant financial support for this work that could have influenced its outcome.

Acknowledgements

The authors acknowledge the support of the European Research Council through project Grant Agreement no. 247045 entitled “Optimization of Multi-scale Structures with Applications to Morphing Aircraft”.

References

[1] I.H. Abbott, A.E. Von Doenhoff, Theory of Wing Sections: Including a Summary of Airfoil Data, Dover Publications, 1959.
[2] M.J. Abzug, E.E. Larrabee, Airplane Stability and Control: A History of the Technologies that Made Aviation Possible, vol. 14, Cambridge University Press, 2005.
[3] ANSYS, Release 11.0 Documentation for ANSYS, ANSYS, Inc., 2007.
[4] S. Barbarino, O. Bilgen, R.M. Ajaj, M.I. Friswell, D.J. Inman, A review of morphing aircraft, J. Intell. Mater. Syst. Struct. 22 (9) (2011) 823–877.
[5] L.F. Campanile, S. Anders, Aerodynamic and aeroelastic amplification in adaptive belt-rib airfoils, Aerosp. Sci. Technol. 9 (1) (2005) 55–63.
[6] I. Chopra, Review of state of art of smart structures and integrated systems, AIAA J. 40 (11) (2002) 2145–2187.
[7] D. Coutu, V. Brailovski, P. Terriault, Optimized design of an active extrados structure for an experimental morphing laminar wing, Aerosp. Sci. Technol. 14 (7) (2010) 451–458.
[8] S. Daynes, P.M. Weaver, Design and testing of a deformable wind turbine blade control surface, Smart Mater. Struct. 21 (10) (2012) 105019.
[9] A. De Gaspari, S. Ricci, A two-level approach for the optimal design of morphing wings based on compliant structures, J. Intell. Mater. Syst. Struct. 22 (10) (2011) 1091–1111.
[10] K. Deb, Multi-Objective Optimization using Evolutionary Algorithms, Wiley-Interscience Series in Systems and Optimization, John Wiley & Sons, Chichester, 2001.
[11] F. Gandhi, P. Anusonti-Inthra, Skin design studies for variable camber morphing airfoils, Smart Mater. Struct. 17 (1) (2008) 015025.
[12] H. Ghiasi, D. Pasini, L. Lessard, Optimum stacking sequence design of composite materials. Part I: constant stiffness design, Compos. Struct. 90 (1) (2009) 1–11.
[13] H. Ghiasi, K. Fayazbakhsh, D. Pasini, L. Lessard, Optimum stacking sequence design of composite materials. Part II: variable stiffness design, Compos. Struct. 93 (1) (2010) 1–13, http://dx.doi.org/10.1016/j.compstruct.2010.06.001.
[14] Z. Gurdal, B. Tatting, C. Wu, Variable stiffness composite panels: effects of stiffness variation on the in-plane and buckling response, Composites, Part A, Appl. Sci. Manuf. 39 (5) (2008) 911–922, http://dx.doi.org/10.1016/j.compositesa.2007.11.015.
[15] H. Haddadpour, Z. Zamani, Curvilinear fiber optimization tools for aeroelastic design of composite wings, J. Fluids Struct. 33 (2012) 180–190.
[16] D.H. Hodges, Nonlinear Composite Beam Theory, American Institute of Aeronautics and Astronautics, 2006.
[17] S. Honda, T. Igarashi, Y. Narita, Multi-objective optimization of curvilinear fiber shapes for laminated composite plates by using NSGA-II, Composites, Part B, Eng. 45 (1) (2013) 1071–1078.
[18] C. Kasapoglou, Design and Analysis of Composite Structures: With Applications to Aerospace Structures, Wiley, 2010.
[19] D. Li, S. Guo, J. Xiang, Modeling and nonlinear aeroelastic analysis of a wing with morphing trailing edge, Proc. Inst. Mech. Eng., G J. Aerosp. Eng. 227 (4) (2012) 619–631.
[20] S. Murugan, M.I. Friswell, Morphing wing flexible skins with curvilinear fiber composites, Compos. Struct. 99 (2013) 69–75.
[21] S. Murugan, R. Ganguli, Aeroelastic stability enhancement and vibration suppression in a composite helicopter rotor, J. Aircr. 42 (4) (2005) 1013–1024.
[22] S. Murugan, R. Ganguli, D. Harursampath, Aeroelastic response of composite helicopter rotor with random material properties, J. Aircr. 45 (1) (2008) 306–322.
[23] S. Murugan, D. Harursampath, R. Ganguli, Material uncertainty propagation in helicopter nonlinear aeroelastic response and vibration analysis, AIAA J. 46 (9) (2008) 2332–2344.
[24] S. Murugan, E.I. Saavedra Flores, S. Adhikari, M.I. Friswell, Optimal design of variable fiber spacing composites for morphing aircraft skins, Compos. Struct. 94 (5) (2012) 1626–1633, http://dx.doi.org/10.1016/j.compstruct.2011.12.023.
[25] M.S. Murugan, B.K.S. Woods, M.I. Friswell, Morphing helicopter rotor blade with curvilinear fiber composite, in: 38th European Rotorcraft Forum, Amsterdam, Netherlands, 4–7 September 2012.
[26] M.A. Nik, K. Fayazbakhsh, D. Pasini, L. Lessard, Surrogate-based multi-objective optimization of a composite laminate with curvilinear fibers, Compos. Struct. 94 (8) (2012) 2306–2313, http://dx.doi.org/10.1016/j.compstruct.2012.03.021.
[27] D.P. Raymer, Aircraft Design: A Conceptual Approach, vol. 3, American Institute of Aeronautics and Astronautics, 1999.
[28] G. Seber, E. Sakarya, Nonlinear modeling and aeroelastic analysis of an adaptive camber wing, J. Aircr. 47 (6) (2010) 2067.
[29] J. Shen, M. Yang, I. Chopra, Swashplateless helicopter rotor with trailing-edge flaps for flight and vibration control, J. Aircr. 43 (2) (2006) 346–352.
[30] A.Y.N. Sofla, S.A. Meguid, K.T. Tan, W.K. Yeo, Shape morphing of aircraft wing: Status and challenges, Mater. Des. 31 (3) (2010) 1284–1292, http://dx.doi.org/10.1016/j.matdes.2009.09.011.
[31] C. Thill, J. Etches, I. Bond, K. Potter, P. Weaver, Morphing skins, Aeronaut. J. 112 (1129) (2008) 117–139.
[32] G. Thuwis, M. Abdalla, Z. Gurdal, Optimization of a variable-stiffness skin for morphing high-lift devices, Smart Mater. Struct. 19 (12) (2010) 124010.

[33] V.V. Volovoi, D.H. Hodges, C.E. Cesnik, B. Popescu, Assessment of beam modeling methods for rotor blade applications, Math. Comput. Model. 33 (10) (2001) 1099–1112.
[34] B.K.S. Woods, M.I. Friswell, Preliminary investigation of a fishbone active camber concept, in: Proceedings of the ASME 2012 Conference on Smart Materials, Adaptive Structures and Intelligent Systems, Stone Mountain, GA, 2012.
[35] B.K.S. Woods, M.I. Friswell, Fluid–structure interaction analysis of the fish bone active camber mechanism, in: 54th AIAA/ASME/ASCE/AHS/ASC Structures, Structural Dynamics, and Materials Conference, Boston, Massachusetts, USA, 2013.
[36] XFOIL, version 6.96, MIT, Cambridge, MA, USA, 2005.
[37] W. Yin, Stiffness requirement of flexible skin for variable trailing-edge camber wing, Sci. China, Technol. Sci. 53 (4) (2010) 1077–1081.